NASA Technical Paper 1097

Secondary-Electron-Emission Properties of Conducting Surfaces With Application to Multistage Depressed Collectors for Microwave Amplifiers

Ralph Forman

NOVEMBER 1977

NASA

Secondary-Electron-Emission Properties of Conducting Surfaces With Application to Multistage Depressed Collectors for Microwave Amplifiers

Ralph Forman
Lewis Research Center
Cleveland, Ohio

SECONDARY-ELECTRON-EMISSION PROPERTIES OF CONDUCTING

SURFACES WITH APPLICATION TO MULTISTAGE DEPRESSED

COLLECTORS FOR MICROWAVE AMPLIFIERS

by Ralph Forman

Lewis Research Center

SUMMARY

Attaining the highest possible efficiencies from multistage depressed collectors requires the use of low-secondary-electron-yield surfaces for electrodes. Coating copper surfaces with low-yield soot has been shown to improve the collector efficiency by 2 to 4 percentage points over an octave bandwidth and, in some cases, the overall tube efficiency by an even higher percentage. Since soot is not a practical solution to this problem because of its poor adhesion properties, the secondary-emission characteristics of a number of materials that are possible candidates for collector electrodes were investigated.

The materials studied were beryllium, carbon (soot and pyrolytic graphite), copper, titanium carbide, and tantalum. Both total secondary yield δ (ratio of total secondary current to total primary current) and relative reflected-primary yield were measured. These measurements were made in conjunction with Auger spectroscopy so that the secondary-emission characteristics could be determined as a function of surface contamination or purity. The measurements show that low-atomic-weight elements, such as beryllium and carbon, have the lowest reflected-primary yield and that roughening the surface of an electrode can markedly decrease the secondary yield for both δ and the reflected primaries. It was found that a roughened pyrolytic graphite surface shows the greatest potential for improving the efficiency of depressed collectors.

INTRODUCTION

In recent years there has been considerable interest in the use of multistage depressed collectors for microwave tubes. Their use has led to a marked improvement in the efficiency and performance of microwave tubes for use in both space and military applications (ref. 1). The Lewis Research Center has been a pioneer in these investi-

gations (refs. 2 and 3) and is still actively engaged in this field (ref. 1). An important parameter in the design of depressed collectors is the secondary yield (including reflected primaries) of the collector surfaces. The lower the secondary yield, the more efficient the device will be. Although copper has been extensively used because it has excellent electrical and thermal characteristics, it is known to have a relatively high secondary yield (ref. 4). To overcome this difficulty, soot, which has low secondary yield (refs. 5 and 6), has been deposited on copper collectors to improve their performance. This has been successful. However, soot is a poor practical choice for use on depressed collectors because of its poor adhesion and mechanical properties. In an attempt to find a more suitable material with a low secondary yield, this investigation was begun.

Secondary-electron emission is the effect in which electrons are emitted from a solid when its surface is bombarded with electrons (ref. 4). The effect has been studied for more than 50 years, and the data are voluminous but not always reliable or reproducible. The early work particularly suffered from these faults and most of the difficulty arose from the poor vacuum conditions that were prevalent at the time. Since the early 1950's, with the introduction of ultra-high-vacuum techniques, these types of measurements have been more reliable but they still suffered from the inability to know just how clean the surface being investigated was. With the development of new surface study techniques in recent years (e.g., Auger spectroscopy (ref. 7) and ESCA (ref. 8), this problem can be ameliorated. The chemical constitution of a solid surface can now be readily evaluated in conjunction with other surface measurements. Thus, we can now measure secondary-electron emissions from solid surfaces, knowing the chemical species on the surface. This is the technique used in the present experiment, which consists of making secondary-emission measurements in conjunction with Auger electron spectroscopy (AES). Both the secondary-emission ratio δ and the relative magnitudes of the reflected primaries were measured over the primary-electron energy range of 300 to 2000 volts.

Measurements were made on the elements beryllium, carbon (pyrolytic graphite and soot), copper, and tantalum. Titanium carbide, which has been reported to have a low secondary yield (refs. 4 and 9), was also studied. Earlier investigations have shown that roughening the surface leads to lower secondary yields (refs. 4 and 10). This avenue of pursuit was also followed. The surfaces of copper and graphite samples were roughened by controlled sputtering techniques, and their surface properties were compared with the original surface properties. On copper, a sputtering technique produced surface cones that varied from 1 to 25 micrometers in diameter. On pyrolytic graphite, needle-like spikes about 1 micrometer in diameter were generated.

BACKGROUND INFORMATION

A depressed collector is used in a linear-beam microwave amplifier tube to slow down the electron beam used to magnify radiofrequency (rf) signals and to collect the electrons at low energies to minimize the energy dissipated in the collection process. The electron beam of the microwave tube is confined magnetically and reacts with the rf wave in the circuit part of the tube. After it has accomplished its mission in the rf circuit part of the tube, the electron beam is allowed to expand into the collector portion of the tube by removing the confining magnetic field at the entrance of the collector structure. Under these circumstances, the electron beam diverges as illustrated in figure 1. Typical depressed-collector geometry and voltages are illustrated, where $-V_0$ is the cathode potential. The electrons are slowed by the retarding electric field set up by the depressed collector.

The trajectories shown in figure 1 are symmetrical; but, for simplicity, only the right sides are shown in the figure. The most energetic electrons are collected by the top electrode, and the less energetic ones are collected by the lower electrodes. For a typical design the average energy at which the electrons are collected by their respective collectors is computed to be about 1000 eV. If the electrons were to hit, and be completely absorbed by, the electrodes, the collector would be highly efficient. However, all electrical conducting surfaces are not perfect absorbers. In fact, many of them may be efficient secondary emitters. If the surface has a high secondary yield, the collector efficiency is lowered.

This principle is illustrated in figure 1, where four different trajectories are shown. The most energetic electrons hit the top plate, shown by trajectory a. Most of the electrons are collected on the tops of the electrodes, as illustrated by trajectories b and d; but some do hit the bottom of an electrode, as illustrated by trajectory c. Secondary electrons that come off a conducting surface have the following energy distribution characteristics. Two large peaks occur in the energy distribution: one is present at 0 to 50 electron volts and represents the true secondaries, and the other occurs near the primary bombarding voltage and results from reflected primaries. True secondaries that come off the surface as a result of trajectories b and d are retarded by the electric field and return to their respective collectors with little loss of energy. However, true secondaries that come from trajectories a and c are accelerated by the electric field and end up at lower collectors with an additional resultant loss in energy, which decreases the efficiency of the depressed-collector system. If reflected primaries are generated, all the trajectory examples will show significant energy losses. The losses are obvious for trajectories a and c, but they also occur for trajectories b and d. For trajectories b and d the reflected primaries may come off the surface with energies sufficiently high to escape the confining electric field and find themselves in an accelerating field, with a resultant additional energy loss. In both cases, for true secondaries and reflected pri-

3

maries, the losses are undesirable; but reflected primaries obviously represent a larger loss mechanism per electron than secondaries and should be minimized. The loss mechanisms associated with both reflected primaries and true secondaries illustrate the need to lower secondary-emission effects from electron-collecting surfaces in microwave tubes in order to improve the efficiency of such devices. The purpose of the research program described in this report is to accomplish this goal.

EXPERIMENTAL TECHNIQUES

The experimental apparatus used to make the measurements is illustrated in figure 2. Figure 2(a) shows the sample structure used in the experiment. It is a disk about 2.5 centimeters in diameter. Area A is generally the original metallic surface, and area B is either a coating on the surface (e.g., TiC or soot) or a sputtered or roughened original surface. Figure 2(b) illustrates the experimental apparatus. It is enclosed in an all-metal, bakeable, high-vacuum system which uses Vac-Ion pumping and is capable of attaining operating pressures of 1.33×10^{-7} newton per square meter (10^{-9} torr) or less. The sample holder, which holds two samples separated by a ceramic insulator, is held with a micromanipulator that is capable of moving the sample in three dimensions as well as rotating it through 360°. By means of the micromanipulator, either sample can be placed adjacent to either the Auger spectrometer, the ion gun, or the tungsten filament.

Besides being used for identifying chemical species on the surface of the samples, the Auger spectometer was also employed in making secondary-emission measurements. The Auger spectometer is essentially a surface probe that identifies the chemical constituents from the top atomic layers of a surface (ref. 7). It operates on the principle that the energy of the Auger secondary electrons, which are emitted from a surface bombarded with high-energy electrons, in this case, 2000 eV, is related to the atomic levels that are present in the chemical species existing on the surface. An analysis of this spectrum reveals the atomic species on the surface. The tungsten filament and ion gun (fig. 2(b)) were used to degas and clean the surface of the sample: the former by means of electron bombardment heating and the latter by means of ion sputtering. The ion gun, operated in an atmosphere of high-purity argon at 6.65×10^{-3} newton per square meter (5×10^{-5} torr), is capable of removing many surface layers of the parent material by sputtering. Present but not shown in figure 2 was a residual gas analyzer for evaluating any gaseous impurities either in the introduced argon or in the vacuum system.

The technique used for making secondary-emission measurements is illustrated in figure 3. Electrons from the Auger electron gun hit the sample at normal incidence with a primary energy V_p and a current I. The current measured through the sample is I_T; and the secondary current I_s, which comes off the surface, is collected by the

grounded metal vacuum system. The secondary ratio δ for a given primary energy V_p is then given by

$$\delta(V_p) = \frac{I - I_T}{I} \tag{1}$$

As explained previously, the secondary-electron distribution contains two large peaks: one for true secondaries at 0 to 50 eV, and the other for reflected primaries at primary bombarding energy. Eighty to ninety percent of the secondary current is normally from the low-energy true secondaries; the reflected-primary contribution is much lower.

To obtain some data on reflected primaries that could be used to compare the reflected-primary yield from different surfaces, a technique was developed that is illustrated in figure 3. An Auger cylindrical mirror analyzer is used for this purpose. It is an energy analyzer on the secondaries emitted by the sample. The outer cylinder is swept with a sawtooth voltage, as illustrated in figure 3. At a particular voltage V of the outer cylinder, only those secondary electrons having an energy E get through the two grid-like structures in the inner cylinder and are focused and collected in the electron multiplier. By sweeping the outer cylinder with a voltage centered at what corresponds to the primary energy peak, the output of the oscilloscope then displays the signal illustrated in figure 3. The negative peak arises from the capacitative output of the electron multiplier.

The peak-to-peak heights A are taken as the relative magnitude of the reflected-primary current emitted from the surface. Although the A for a given surface is related to the total number of reflected primaries, its usefulness is limited unless it can be interpreted in terms of its relative magnitude as compared with a standard surface. Choosing an appropriate surface standard allows results to be interpreted and compared from measurements on different surfaces. The standard surface used in this study was soot. Soot was chosen because is could be easily deposited on a given surface, as the residue from an oxygen-lean acetylene torch, and because its secondary-emission properties were reproducible. In addition, it had the lowest A of all the surfaces tested in this investigation. To accomplish this goal of always being able to compare the relative magnitude of the reflected-primary parameter A of an unknown sample surface with that of soot, the samples were prepared as shown in figure 2(a). Half the disk was the unknown surface, and the other half was a deposited soot surface. By means of the micromanipulator shown in figure 2(b), successive measurements of A could be made for the unknown surface and then immediately afterward for soot.

5

EXPERIMENTAL RESULTS

The surface properties of a number of materials were studied, all of which could have possible application to improving the efficiency of depressed collectors. Each is individually discussed and the results summarized in this section.

Copper and Sputtered Copper Surfaces

The secondary yields obtained from a copper surface are shown in figure 4. The three curves of δ as a function of primary energy show the change in secondary yield with surface conditions. Curve A is for the copper surface, in the ultra-high-vacuum system, before the surface was degassed or ion cleaned. Curve B was taken on the same surface area after it had been degassed at 600° C for 1 hour. After degassing the surface was ion cleaned and about 1 micrometer of material removed to obtain a clean copper surface; curve C resulted. It is obvious from these curves that the secondary-emission ratio for a copper surface can vary considerably depending on the apparent surface conditions.

This phenomenon can be better understood by examining the conditions on the surface in all three cases. This is done in a qualitative manner in figure 5, which shows the Auger spectra for surface conditions in figure 4. The abscissa of figure 5 is the energy of the measured Auger electrons; and the ordinate is dN/dE, where N is the number of Auger electrons emitted at energy E. It has been shown that dN/dE is a more sensitive parameter than N for detecting the Auger secondary-electron peaks and that the position of the sharp minima in the dN/dE-against-E curves is the best technique for determining the Auger transition energies of atomic species on the surface. The sharp minima in curve A of figure 5, which corresponds to the copper surface before degassing and ion cleaning, show large carbon and oxygen peaks as well as the copper peaks. In addition, there is some sulfur and chlorine present on the surface. After the surface is heated to 600° C (curve B in fig. 5), the chlorine has disappeared, the oxygen content is slightly lower, and the carbon content is slightly higher. After ion cleaning and removing 1 micrometer of material, very prominent copper peaks appear, there is no sulfur, and these are only traces of carbon and oxygen peaks. Since the Auger spectrum of curve C in figure 5 shows an almost pure copper surface, we assume that curve C in figure 4 is that for pure copper.

The variations of reflected primaries with primary bombarding energy for these different copper surface conditions are illustrated in rows 2 to 4 of table I. Table I summarizes the variation of reflected-primary yield A with primary energy for all the surfaces investigated in this study. The values for A are in arbitrary units, but the data are normalized so that the A value for soot at 1000 eV is unity. Since, as explained

6

previously, the reflected-primary yield A of all the surfaces investigated was measured relative to soot, whose values are given in row 1 of table I, they can be quantitatively evaluated against soot as the standard surface. Three data points were always taken in these measurements at primary energies of 500, 1000, and 2000 eV. The most interesting feature of the reflected-primary data for copper is the large number of reflected primaries scattered from a pure copper surface as compared with those from surfaces containing some carbon and oxygen surface contamination. For example, at 1000 eV, the A value of pure copper is about 40 times greater than that of soot.

The secondary-emission characteristics of copper are not the best ones for use in depressed collectors. Surfaces with a secondary yield of 0.5 or lower and a low reflected-primary coefficient A would be much better. However, since copper does have some other desirable characteristics (e.g., ease of fabrication and high thermal and electrical conductivity), attempts have been made to improve the secondary-emission character of a copper surface by roughening the surface in a prescribed manner (ref. 10).

The technique used in preparing the roughened samples has been reported elsewhere (ref. 11) and consists of ion beam texturing a copper base material with a xenon ion source. The technique used in preparing the roughened samples has been reported else- and consists of ion beam texturing a copper base material with a xenon ion source while simultaneously depositing tantalum on the surface of the base copper material. As a result, cones or needle-like protuberances can be formed that are primarily copper but contain some surface deposits of tantalum. The resulting surface texture is illustrated in figure 6: cone formation in figure 6(b) and needle-like protuberances in figure 6(c). The cone diameters in figure 6(b) are about 10 micrometers; the needle diameters in figure 6(c) are less than 1 micrometer.

Figure 7 illustrates the atomic species on the sputtered surface (fig. 6(c)) during the various phases of treatment of the surface. Before the surface is degassed and ion cleaned, the Auger spectrum shows the presence of tantalum, carbon, and oxygen, and possibly copper. After degassing at 600° C for 1/2 hour, the Auger spectrum shows tantalum, a prominent carbon peak, a lower oxygen peak, and no observable copper. Apparently, heating the sample has brought carbon to the surface. The surface of the sample was then ion cleaned by removing approximately 10^{-5} centimeter of the surface, and the Auger spectrum C was obtained. After ion cleaning, tantalum and copper are obviously present on the surface, as well as carbon and oxygen.

The effect of the figure 7 surface changes on secondary-emission characteristics are illustrated by the data in figure 8 and in lines 5-7 of table I. After the surface was degassed, the secondary yield dropped to 0.4 to 0.5, which is very desirable. But after ion cleaning, the effect of reflected primaries increased considerably. It is obvious from comparing data of figures 4 and 8 that roughening the surface lowered the secondary yield characteristics (both secondary electrons and reflected primaries) of the surface. A lower yield was obtained also from a sputtered copper surface with cone-like projections,

as is depicted in figure 6(b). The secondary-emission data from the surface of figure 6(b) were very similar to those presented for the surface of figure 6(c). The role of tantalum in affecting the secondary-emission characteristics of the surface is not clear from the data presented to this point. To evaluate secondary-emission effects of tantalum on the surface, the yield for pure tantalum surfaces was determined, as described in the following section.

Tantalum Surface

When the tantalum surface was studied before degassing or ion cleaning, Auger spectrum A in figure 9 was obtained. In this instance, the surface showed considerable carbon and oxygen but no tantalum. After the surface was degassed at 600° C for 2 hours, spectrum B in figure 9 was obtained; it again shows carbon and oxygen, but now tantalum is also prominent. After the surface was ion bomdarded to remove a few micrometers of metal from the surface, Auger spectrum C in figure 9 was obtained. Tantalum is now the most prominent element, but some carbon and oxygen are still present even after so much material was removed. Because of the high chemical affinity of tantalum, we assume the oxygen and carbon are chemically bonded to the tantalum throughout its volume.

The δ-against-primary-electron-energy curves for these three surface conditions are shown in figure 10. The relatively pure tantalum surface (curve C in fig. 9) has a δ between 0.8 and 0.9. Its reflected-primary characteristics, as given in row 8 of table I, show that it varies from 14 to 68 times greater than soot in the primary-electron energy range 500 to 2000 eV. It is obvious that the presence of tantalum could not have contributed to lowering the secondary yield of the roughened copper surface in figure 6(c) because the tantalum yield values are so high themselves. This is additional collaborating evidence of the well-known principle that roughening the surface of a material lowers its secondary yield.

Beryllium Surfaces

Beryllium is another element that has been reputed to have low secondary yields and it was, therefore, an excellent candidate for this study. A scanning electron micrograph of the beryllium surface is shown in figure 11. Beryllium is extremely brittle, and the black holes represent material torn from the surface when it was prepared. The Auger spectra in figures 12 and 13 illustrate the chemical species on the beryllium surface for given surface conditions. Figures 12 and 13 describe two different energy range spectra for the same surface conditions, given by curves A, B, and C. The characteristic Auger transition for pure beryllium is about 105 eV; when the surface is oxidized, the transition level drops to 95 eV from its original value (ref. 12). By this technique, we can readily

distinguish between beryllium and beryllium oxide on the surface, and its application is aptly illustrated by figures 12 and 13.

Auger spectra of the untreated surfaces are shown in curves A of figures 12 and 13. These curves show that beryllium oxide, carbon, and oxygen are initially present on the surface. Spectra of the surface after it had been degassed at 600° C for about 2 hours are shown in curves B of figures 12 and 13. The Auger spectra have been changed by the degassing and now show both beryllium and beryllium oxide on the surface. In addition, carbon is still present, but the oxygen content of the surface has decreased. Further treatment of the surface by argon ion cleaning and removing about 5×10^{-6} centimeter of material from the surface results in spectra C of figures 12 and 13. These curves now show that, except for some very minor impurities of argon, carbon, and oxygen on the surface, unoxidized beryllium is the only major element present.

The variation of δ with electron energy for these beryllium surfaces is shown in figure 14.

The top curve combines the data for the untreated surfaces (figs. 12 and 13, curves A) and those for the outgassed surfaces (figs. 12 and 13, curves B). Heat treatment did not change the secondary-emission ratio at all. However, when about 5×10^{-6} centimeter of material was removed from the surface to eventually get a clean beryllium surface (figs. 12 and 13, curves C), the bottom curve in figure 14 was obtained. A pure beryllium surface causes a very significant decrease in δ. The data on reflected primaries follow a different pattern. The results, in this case, were independent of the surface treatment.

Row 9 in table I gives the data obtained from a clean beryllium surface (e. g., spectrum C of fig. 12). The data for an untreated surface agree with the magnitude of reflected primary yield to ±0.3, which is in the range of accuracy for these measurements. Comparing the reflected-primary data for beryllium in table I with the clean copper and tantalum data shows that beryllium has a much lower reflected-primary yield than either copper or tantalum.

Titanium Carbide Surfaces

Some metal carbides, including titanium carbide, have relatively low secondary yields (ref. 9). For this reason, titanium carbide, as one example of this class of materials, was investigated. The titanium carbide sample[1] was in the form of a layer of titanium carbide on a copper substrate and looked like the sample in figure 2(a), with copper present in area A and titanium carbide in area B. To the eye the titanium carbide surface was black. On a submicroscopic range, a scanning electron micrograph shows

_____

[1]Obtained through the courtesy of Varian Associates, Palo Alto, Calif.

the rugged landscape of figure 15. The Auger spectrum for the surface, after degassing and ion cleaning, is shown in figure 16. Since argon ions were used to sputter clean the surface, their presence is understandable. However, the large oxygen peak is not easily explained. It persists even after removal of 1 micrometer of surface, and it probably arises from the fabrication technique used in producing the titanium carbide layer.

The secondary-emission data for the titanium carbide surface of figures 15 and 16 are shown in figure 17 and line 10 of table I. The δ values vary from 0.5 to 0.6 in the range 300 to 2000 eV, but the reflected-primary values for titanium carbide are about 10 times larger than that for soot.

Carbon Surfaces

Carbon is of particular interest because in its most simple form, soot, it seems to have the best qualities of a low-secondary-yield material (ref. 5). Under these circumstances, it would appear that other forms of carbon that are more practical, such as pyrolytic graphite, would be of pragmatic interest. This is the major subject of this section.

Before the studies on pyrolytic graphite are discussed, it would be informative to describe the data obtained on soot. A scanning electron micrograph of soot is shown in figure 18. As expected, it shows no ordered structure on the surface. An Auger spectrum of all the soot surfaces shows only carbon and no other impurities. Measurements of secondary yield from soot show that δ is relatively independent of primary energy in the range 300 to 2000 eV and has a value of approximately 0.4. From the data of table I, soot obviously has the lowest reflected-primary yield of any of the materials tested and therefore meets all the criteria of being an excellent low-secondary-emission surface. This unusual quality probably arises for the following reasons: (1) soot is carbon, and (2) the soot surface is very rough and uneven. Experiments on pyrolytic graphite can give us some insight into the relative effect of both these conditions on the secondary yield.

The Auger spectra obtained from a smooth, basal-plane pyrolytic graphite surface before and after heating and ion cleaning are shown in figure 19. The sulfur and titanium are apparently initial surface contaminants that are easily removed by ion cleaning. The secondary-emission-ratio data (fig. 20) show that higher energy data do not change when the surface is cleaned, but the lower energy data do. Actually, this effect results from just degassing the sample. A curve similar to curve B in figure 20 was obtained from the surface associated with curve A in figure 20 after degassing it at 500° to 600° C for 1 hour. The reflected-primary data of row 11 of table I were identical for all the surface conditions illustrated in figure 19. It shows that pyrolytic graphite also has a low reflected-primary yield (about three times that of soot) and is comparable in that respect to beryllium. Since smooth pyrolytic graphite has a relatively low secondary yield (for both secondaries and reflected primaries), it is apparent that this

property could be further enhanced by roughening the surface. In one instance this was done by sputter etching the surface in an argon atmosphere until the scanning electron micrograph of figure 21 was obtained. Auger spectra of this carbon surface before and after degassing show that the only minor constituent on the surface was oxygen. Secondary-emission data from the sputter-etched surface after degassing the surface are shown in figure 22 and in line 12 of table I. The data were similar before and after degassing. Measurements on soot are also included in figure 22, and they show that the sputter-etched surface of figure 21 is similar to that of soot in its secondary-emission properties. Its δ characteristics are slightly lower than soot, but reflected-primary characteristics are slightly higher. This shows that proper surface treatment of pyrolytic graphite can result in a surface that exhibits extremely low secondary-emission characteristics, comparable to those of soot.

DISCUSSION OF RESULTS

There are a number of interesting observations made in the previous section that deserve further discussion:
(1) Effect of surface contaminants on secondary emission
(2) The low reflected-primary yield of elements like beryllium and carbon
(3) Effect of roughening the surface on secondary emission
Carbon and oxygen are the common contaminants found on the surfaces before they are either degassed or cleaned. An apparent effect of these contaminants is to decrease the reflected-primary current (table I, lines 2 to 7). The following explanation is presented for this effect: The light atomic elements (e.g., beryllium, carbon, and oxygen) show a very low reflected-primary yield, as described in the following paragraph. When these substances are major constituents of the surface, as seen by the Auger spectra, they must then dominate the reflected-primary effect because the high-energy secondary electrons, whether they be Auger or reflected primaries, are probably generated in a surface layer having the same depth. If this explanation is valid, it easily accounts for the experimental result illustrated in lines 2 to 7 of table I.

Table I shows that the low-atomic-weight elements beryllium and carbon have a markedly lower reflected-primary yield than the cleaned heavy metals copper and tantalum. The effect is so pronounced, experimentally, that on the basis of these limited data one is tempted to predict that the surfaces of low-atomic-weight elements would all have a lower reflected-primary yield than the surfaces of heavy elements. As confirmatory evidence, this hypothesis explains the behavior of oxygen in the beryllium – beryllium oxide experiments. Oxygen on the beryllium surface increases the secondary yield δ considerably from the clean condition (fig. 14). However, the low reflected-primary yield of the beryllium surface is insensitive to the presence of oxygen.

11

It has been well known that the degree of roughness on a surface has a large effect on the emission of secondaries (ref. 13). The present experiments confirm these results. However, in the case of the pyrolytic graphite, where the roughening influence could be separated from any surface impurity effect, the roughening influence on both secondary yield δ and the reflected-primary yield was much more pronounced at low primary energies than at higher ones.

Curves that summarize the data are shown in figures 23 and 24. The information on the elements beryllium, carbon, copper, and tantalum are for the smooth ion-cleaned surface unless otherwise described. The titanium carbide data are for the roughened surface shown in figure 15. These figures show that beryllium and pyrolytic graphite have the lowest secondary-emission characteristics and seem to be obvious candidates for use in devices that require surfaces having a low secondary yield. However, beryllium has one disadvantage with respect to pyrolytic graphite. Any oxygen contamination of the beryllium surface would destroy its usefulness for that purpose because of the large increase in δ. Since in most applications, the surfaces would have to be processed and handled in air, ensuring oxidation, beryllium can be eliminated as a pragmatic choice for any low-secondary-yield application. This leaves pyrolytic graphite as the best material choice in applications requiring low secondary yield. Roughening the surface, as described previously, leads to even further improvement, which makes the pyrolytic graphite surface comparable to soot, without the disadvantages of soot.

CONCLUSIONS

The purpose of this investigation was to develop an electrode surface with a very low secondary yield for use in a depressed collector for high-efficiency traveling wave tubes. In the course of this study, the secondary-emission characteristics of smooth and roughened surfaces of a number of materials that were considered likely candidates for electrodes in a depressed collector were investigated. These included beryllium, carbon (soot and pyrolytic graphite), copper, titanium carbide, and tantalum. The results of these measurements show that roughened pyrolytic graphite is the lowest secondary-yield material for use in depressed collectors. It can be used as a solid electrode material and as such has other advantages besides that of low secondary yield. It exhibits exceptional strength, is easily machineable, and has high thermal conductivity properties when properly oriented ("a" direction).

Lewis Research Center,
    National Aeronautics and Space Administration,
        Cleveland, Ohio, August 1, 1977,
            506-20.

REFERENCES

1. Kosmahl, Henry G.; and Ramins, P.: Small-Size 81- to 83.5-Percent Efficient 2- and 4-Stage Depressed Collectors for Octave-Bandwidth High-Performance TWT's. IEEE Trans. Electron Devices, vol. ED-24, no. 1, Jan. 1977, pp. 36-44.

2. Kosmahl, Henry G.: A Novel, Axisymmetric Electrostatic Collector for Linear Beam Microwave Tubes. NASA TN D-6093, 1971.

3. Kosmahl, H. G.: An Electron Beam Controller. U.S. Patent 3,764,850, Oct. 1973.

4. Gibbons, D. J.: Secondary Electron Emission. Handbook of Vacuum Physics, vol. 2, part 3, A. H. Beck, ed., Pergamon Press, Ltd., 1966, pp. 301-395.

5. Bruining, H.; de Boer, J. H.; and Bergers, W. G.: Secondary Electron Emission of Soot in Valves with Oxide Cathodes. Physica (Utrecht), vol. 4, Apr. 1937, pp. 267-275.

6. Espe, Werner: Carbon Products for High-Vacuum Technique (in German). Vak. Tech., vol. 4, no. 1, Apr. 1955, pp. 10-24; ibid., vol. 4, no. 2, June 1955, pp. 34-40.

7. Chang, Chuan C.: Auger Electron Spectroscopy. Surf. Sci., vol. 25, 1971, pp. 53-79.

8. Siegbahn, K.: Electron Spectroscopy for Chemical Analysis. AFML-TR-68-189, Air Force Materials Laboratory, 1968. (Available from DDC as AD-844315.)

9. Thomas, S.; and Pattinson, E. B.: Automatic Measurement of Secondary Electron Emission Characteristics of TaC, TiC and ZrC. Br. J. Appl. Phys. ser. 2, vol. 2, 1969, pp. 1539-1547.

10. Thomas, S.; and Pattinson, E. B.: The Controlled Preparation of Low SEE Surfaces by Evaporation of Metal Films Under High Residual Gas Pressures. J. Phys. D (Applied Phys.), vol. 3, 1970, pp. 1469-1474.

11. Hudson, Wayne R.: Ion Beam Texturing. NASA TM X-73470, 1976.

12. Suleman, M.; and Pattinson, E. B.: Auger Spectroscopy of Beryllium. J. Phys. F (Metal Phys.), vol. 1, 1971, pp. L24-L27.

13. Rachkovskii, S. F.: Secondary Emissions from Rough Surfaces. Radio Eng. Electron, vol. 3, no. 3, 1958, pp. 97-118.

Surface conductor	Primary energy, eV		
	500	1000	2000
	Magnitude of reflected-primary yield, A		
1 - Soot	1.5	1.0	0.55
2 - Copper surface before degassing	9.3	12.0	10.2
3 - Copper surface after degassing	8.5	10.4	8.4
4 - Copper surface after degassing and ion cleaning	28.0	42.8	30.4
5 - Sputtered copper surface before degassing	3.9	5.1	6.7
6 - Sputtered copper surface after degassing	3.1	3.7	4.9
7 - Sputtered copper surface after degassing and ion cleaning	10.2	12.0	14.9
8 - Tantalum surface after degassing and ion cleaning	20.3	25.0	37.3
9 - Ion-cleaned beryllium surface	3.6	3.1	1.8
10 - Titanium carbide surface	10.0	10.6	6.8
11 - Smooth pyrolytic graphite surface	4.4	3.3	1.8
12 - Sputter-etched pyrolytic graphite surface	1.9	1.8	1.5
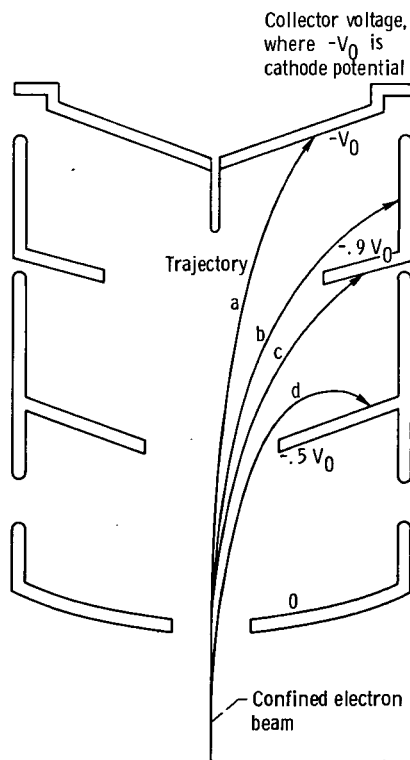
Figure 1. - Depressed-collector configuration for traveling-wave tube.

(a) Disk sample.

Ion gun

Auger spectrometer

Micromanipulator

Electron gun

Tungsten
filament

Sample 1

Ceramic
separator
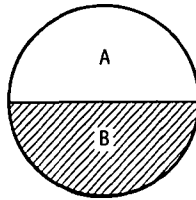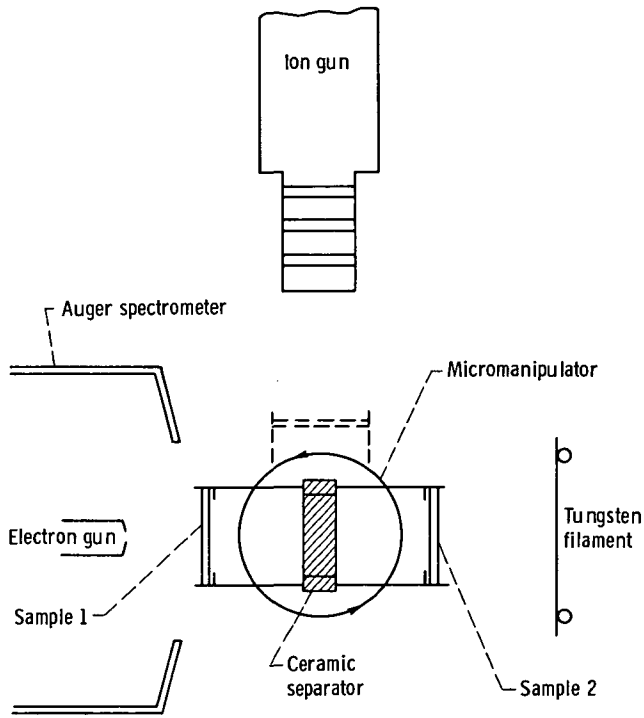
Sample 2

(b) Experimental apparatus.

Figure 2. - Experimental apparatus and disk sample.
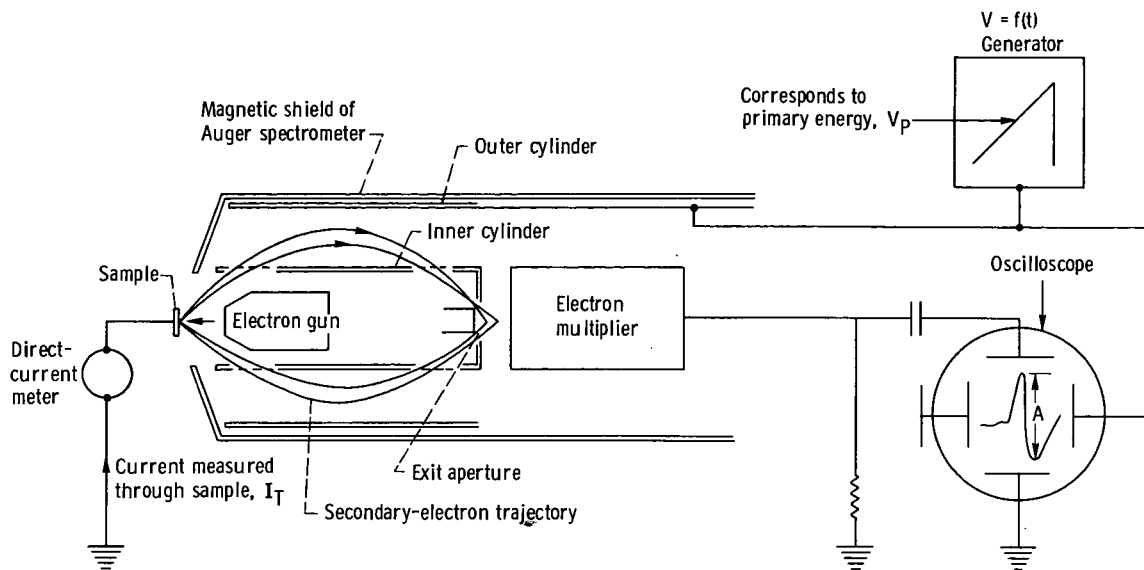
Figure 3. – Secondary-emission measurement equipment.
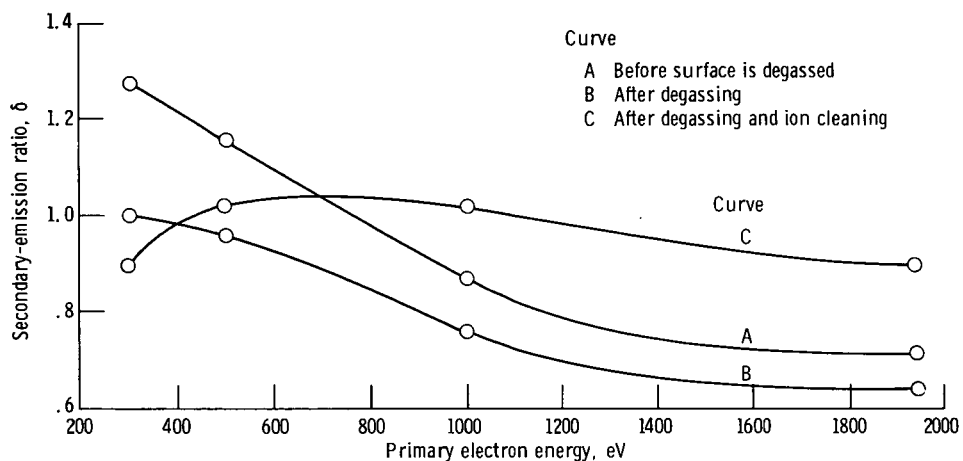
Figure 4. – Secondary-emission ratio as function of primary-electron energy for copper in range 300 to 2000 eV.
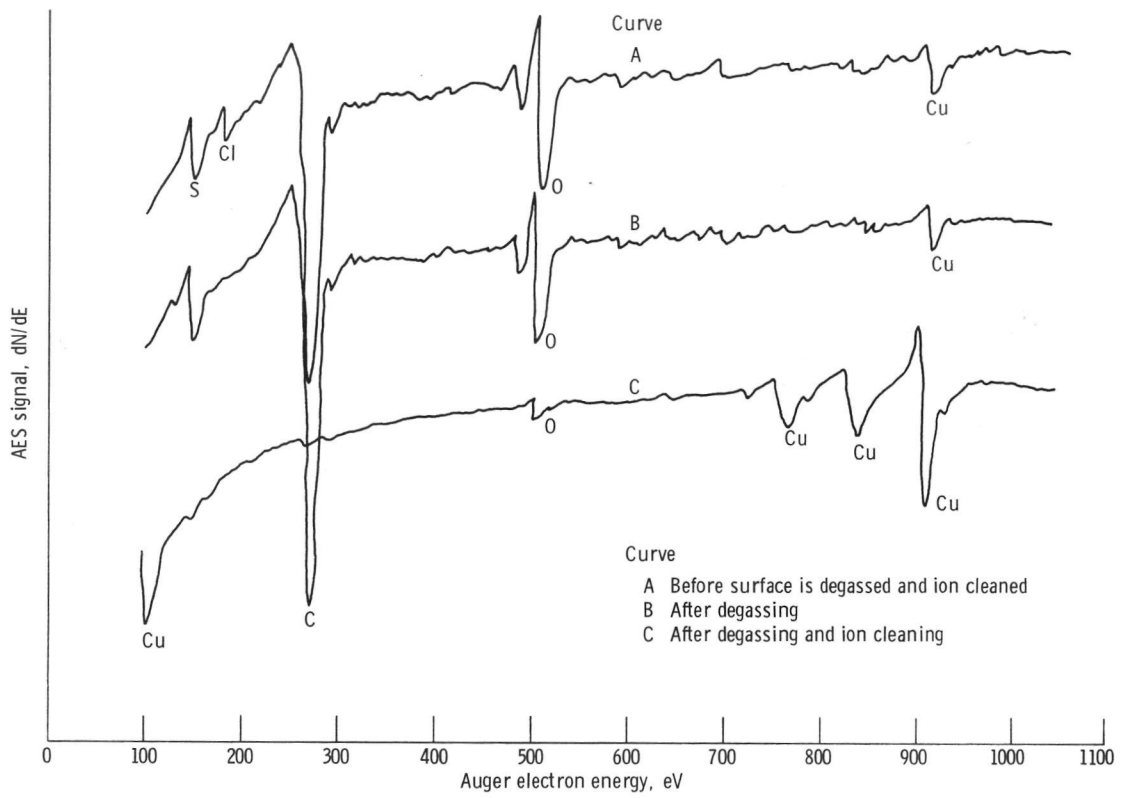
Figure 5. – Auger spectra for copper surface.

(a) As-machined copper surface. X1000.
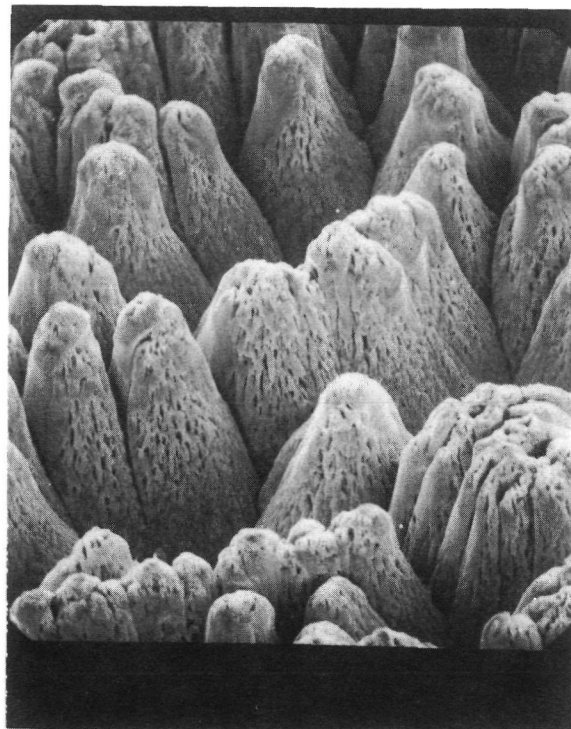
(b) Sputtered copper surface having cones. X1000.

(c) Sputtered copper surface having needle-like
protuberances.

Figure 6. - Scanning electron micrographs of copper surfaces showing texturing.
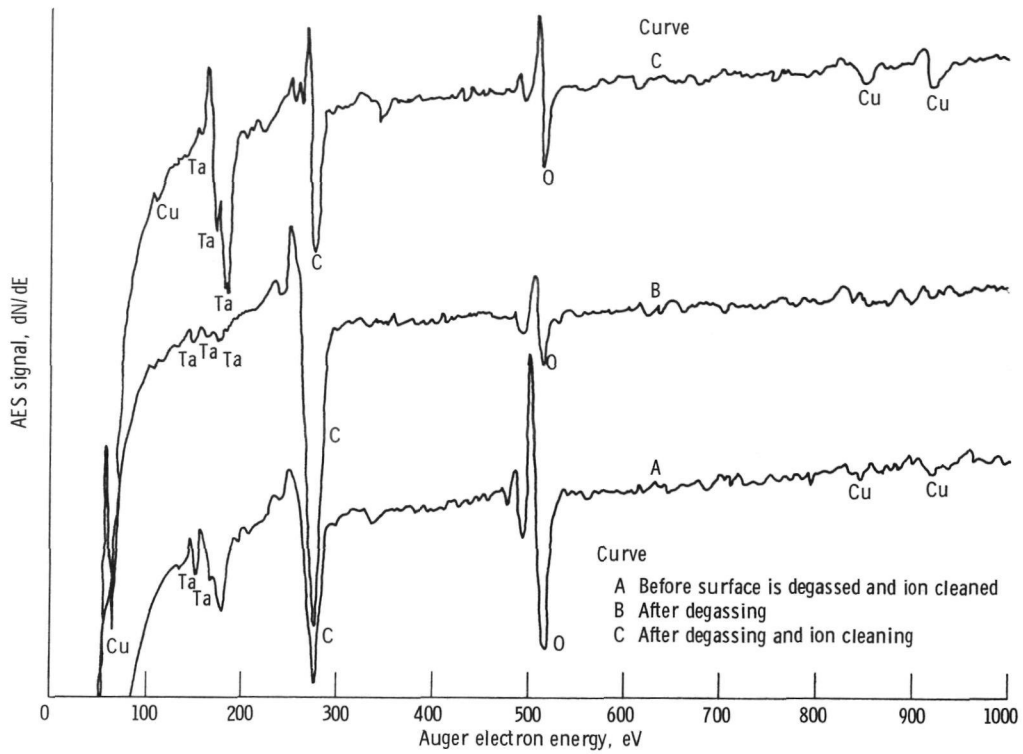
Figure 7. - Auger spectra for sputtered copper surface shown in figure 6(c).
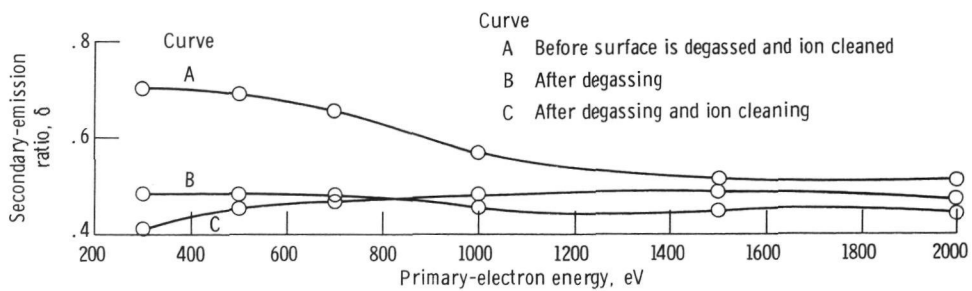
Figure 8. - Secondary-emission ratio as function of primary-electron energy for sputtered copper in range 300 to 2000 eV.
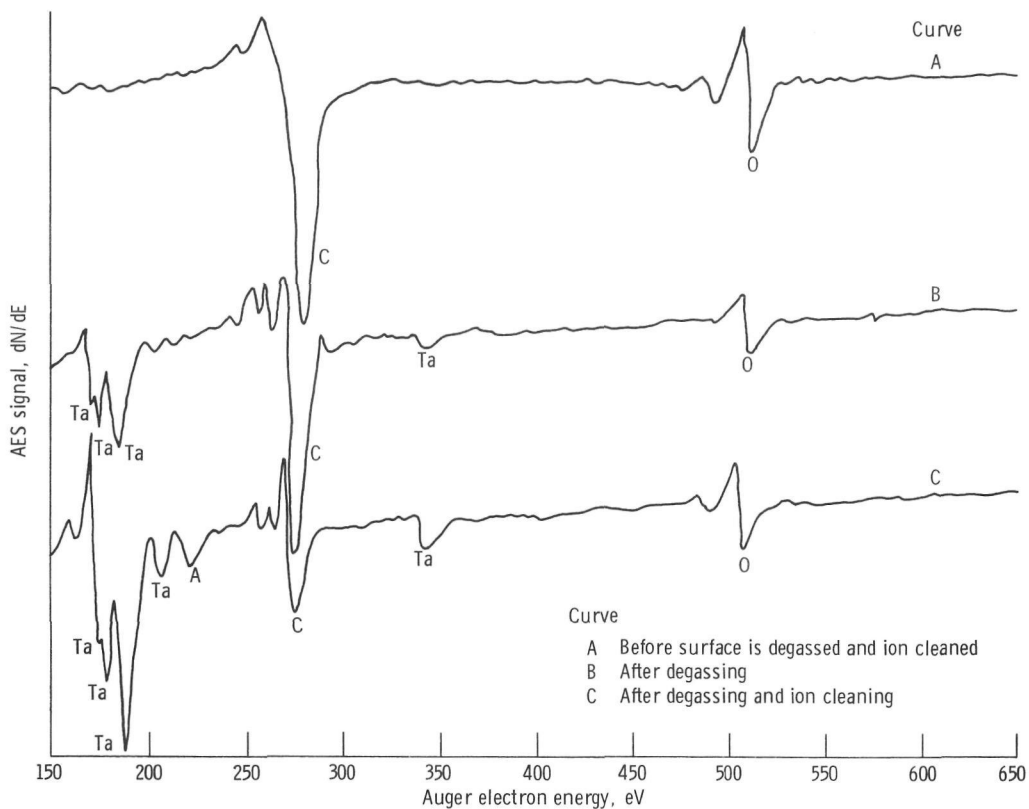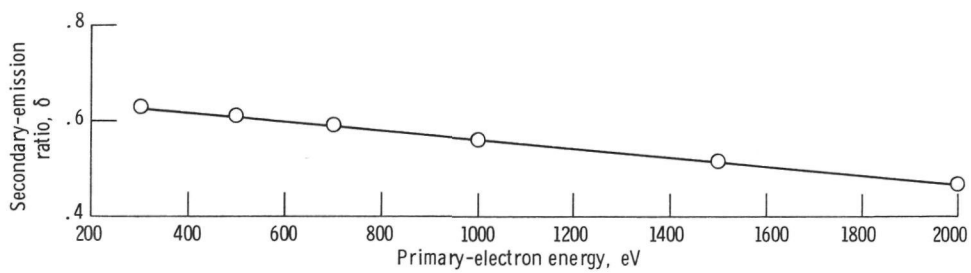
Figure 9. – Auger spectra for tantalum surface.
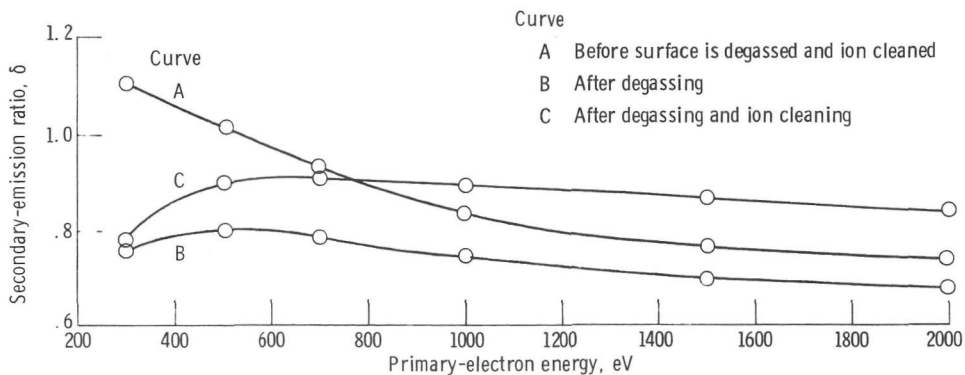
Figure 10. – Secondary-emission ratio as function of primary-electron energy for tantalum surface in range 300 to 2000 eV.
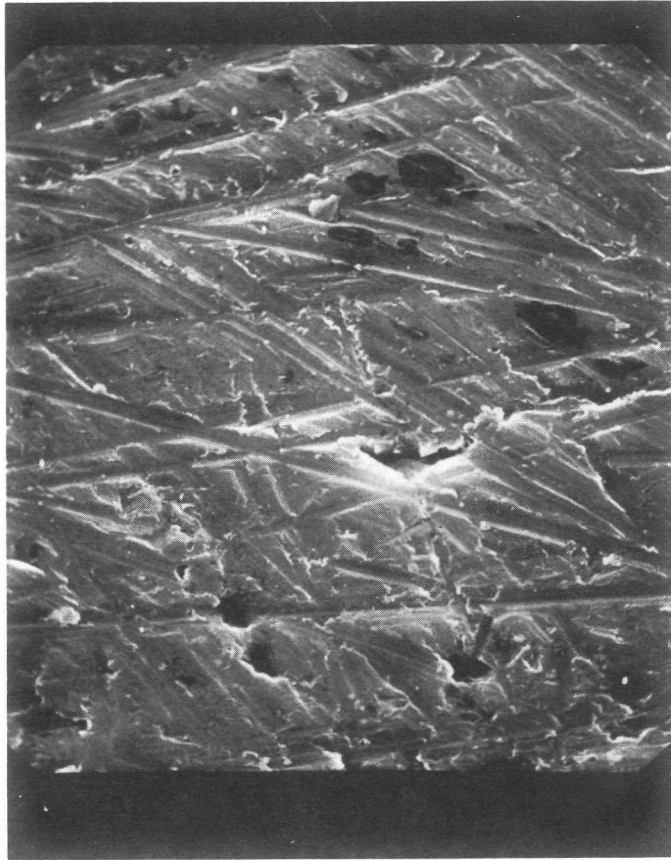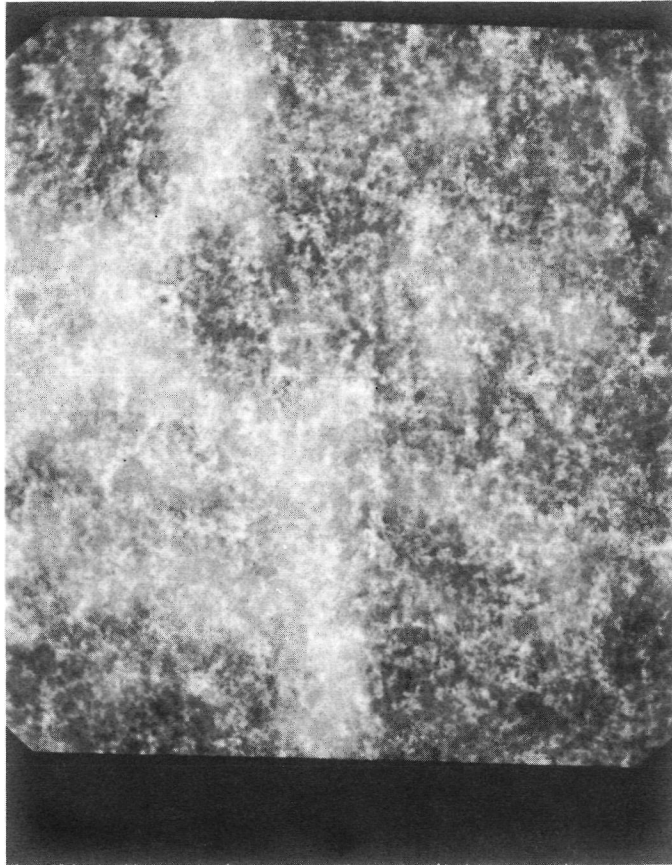
Figure 11. - Scanning electron micrograph of beryllium surface. X1000.
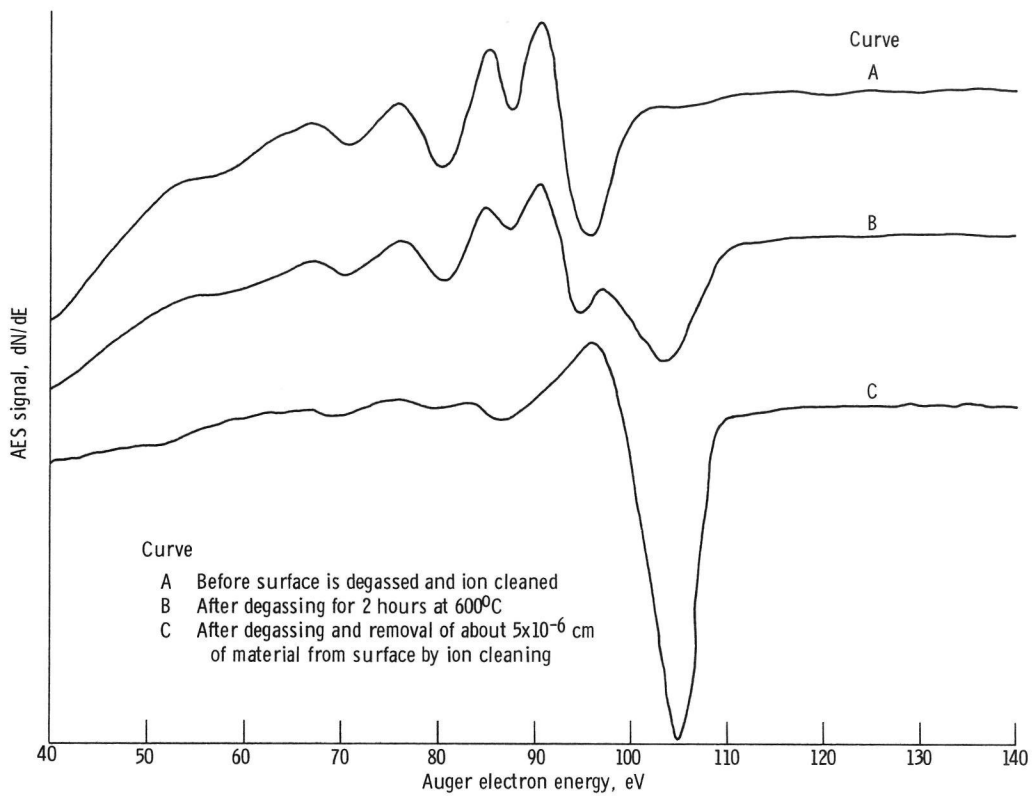
Figure 12. – Auger spectra for beryllium surface in range 40 to 140 eV.
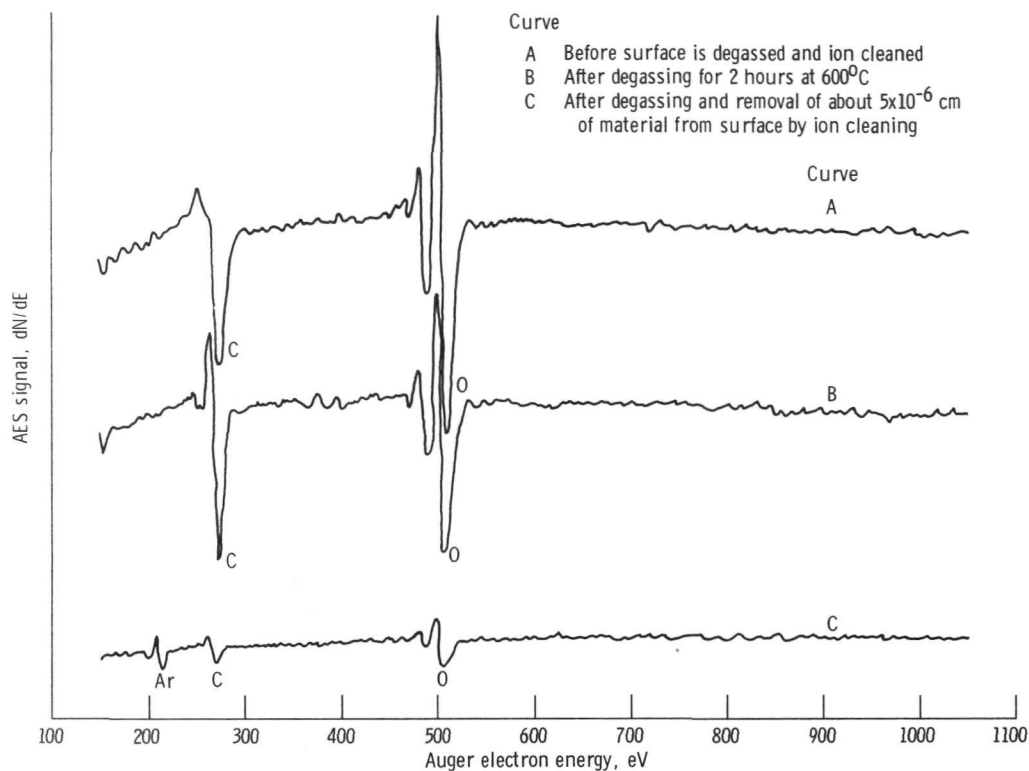
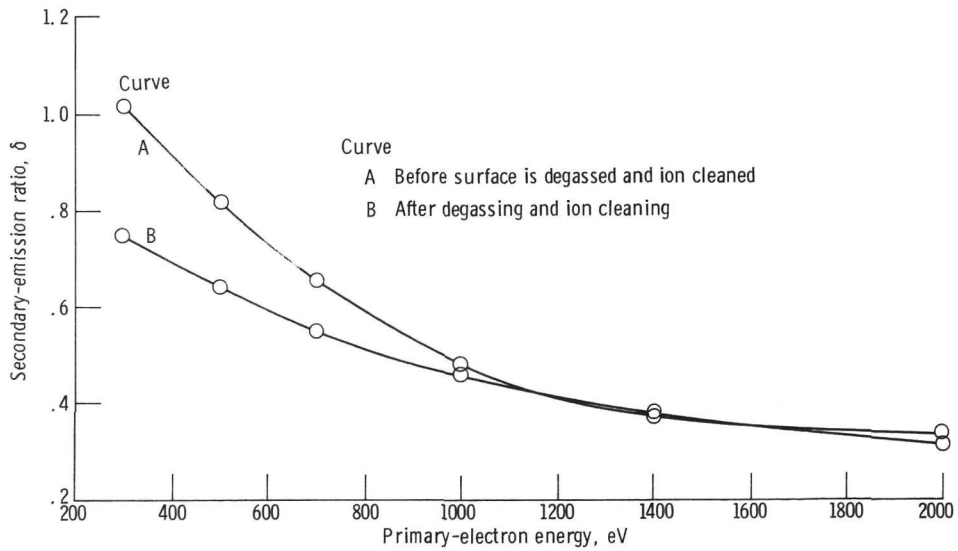Figure 13. - High-energy Auger spectra for beryllium surface in range 150 to 1050 eV.
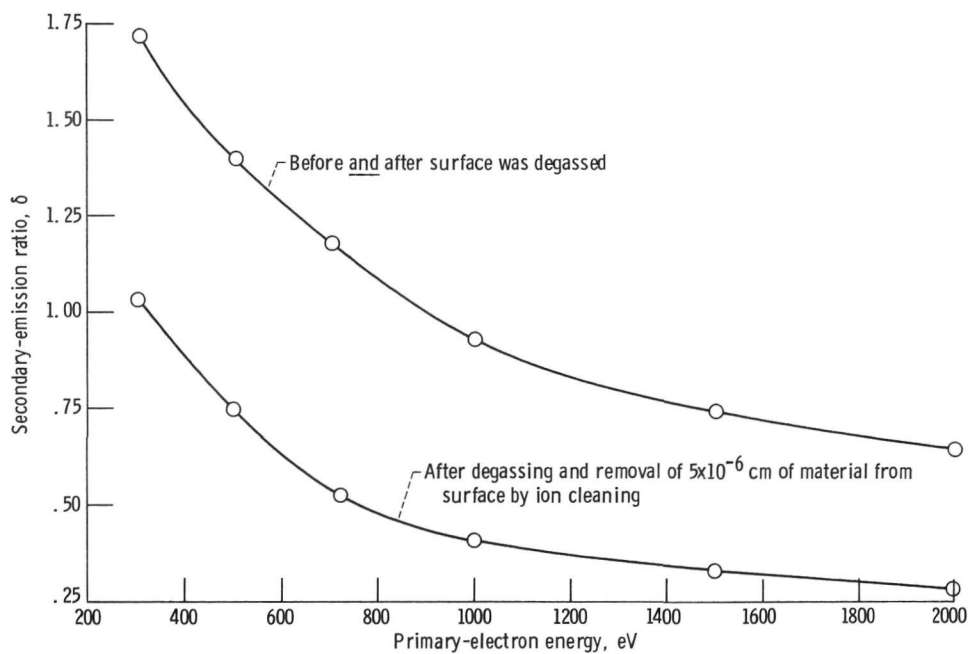
Figure 14. - Secondary-emission ratio as function of primary-electron energy for beryllium surface in range 300 to 2000 eV.
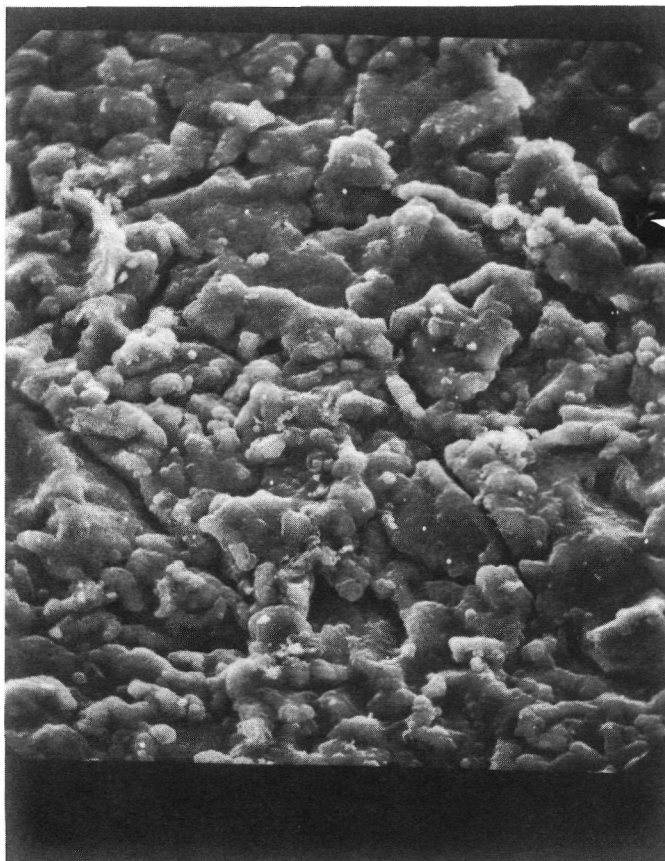
Figure 15. - Scanning electron micrograph of titanium carbide surface. X1000.

24
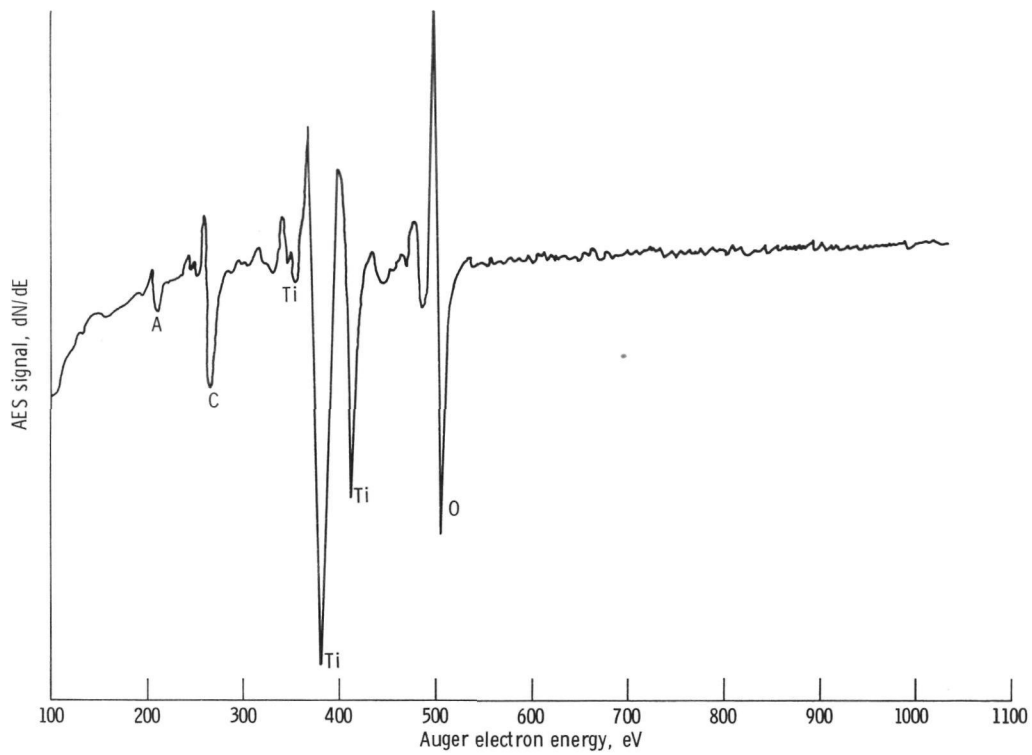
Figure 16. – Auger spectrum for titanium carbide surface degassed and ion cleaned, in range 100 to 1000 eV.

Figure 17. – Secondary-emission ratio as function of primary-electron energy for titanium carbide surface in range 300 to 2000 eV.
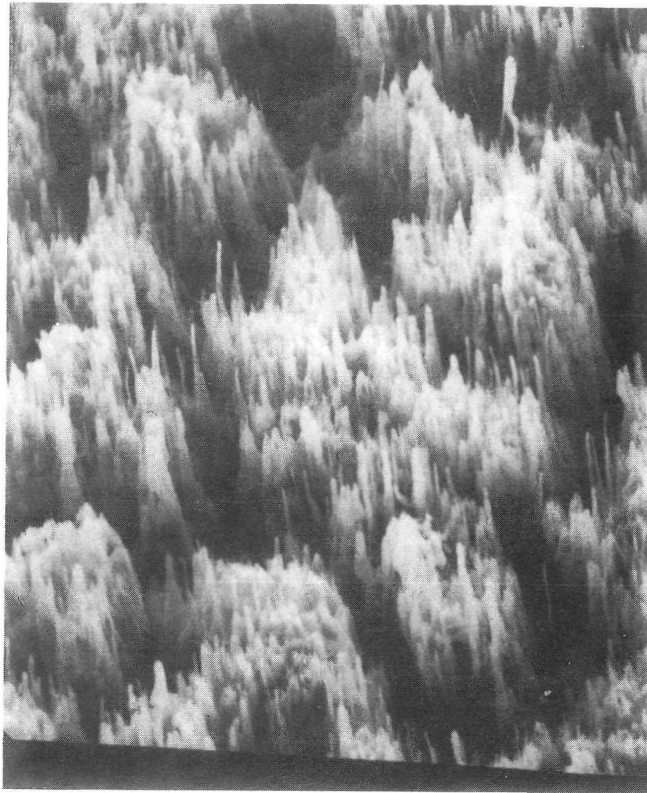
Figure 18. - Scanning electron micrograph of soot surface. X3000.
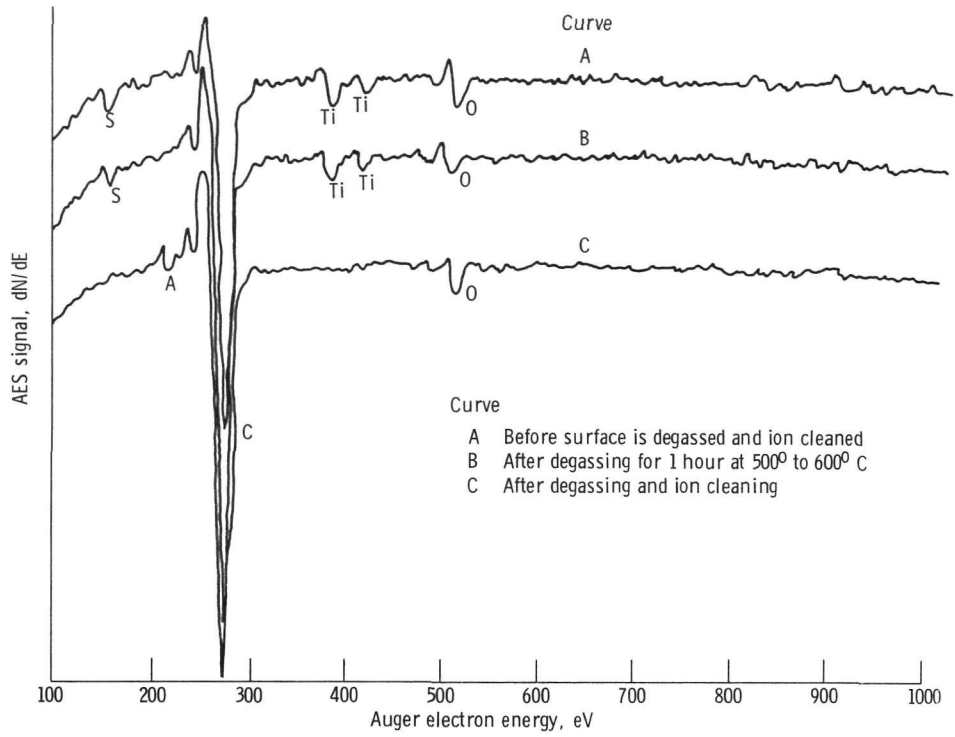
Figure 19. – Auger spectra for smooth pyrolytic graphite surface in range 100 to 1000 eV.

Figure 20. – Secondary-emission ratio as function of primary-electron energy for smooth pyrolytic graphite surface in range 300 to 2000 eV.

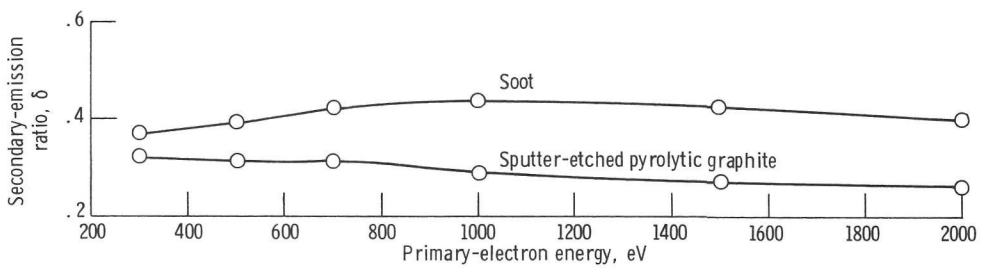Figure 21. - Scanning electron micrograph of sputter-etched pyrolytic graphite surface. X1000.

Figure 22. - Secondary-emission ratio as function of primary-electron energy for sputter-etched pyrolytic graphite and soot surfaces.
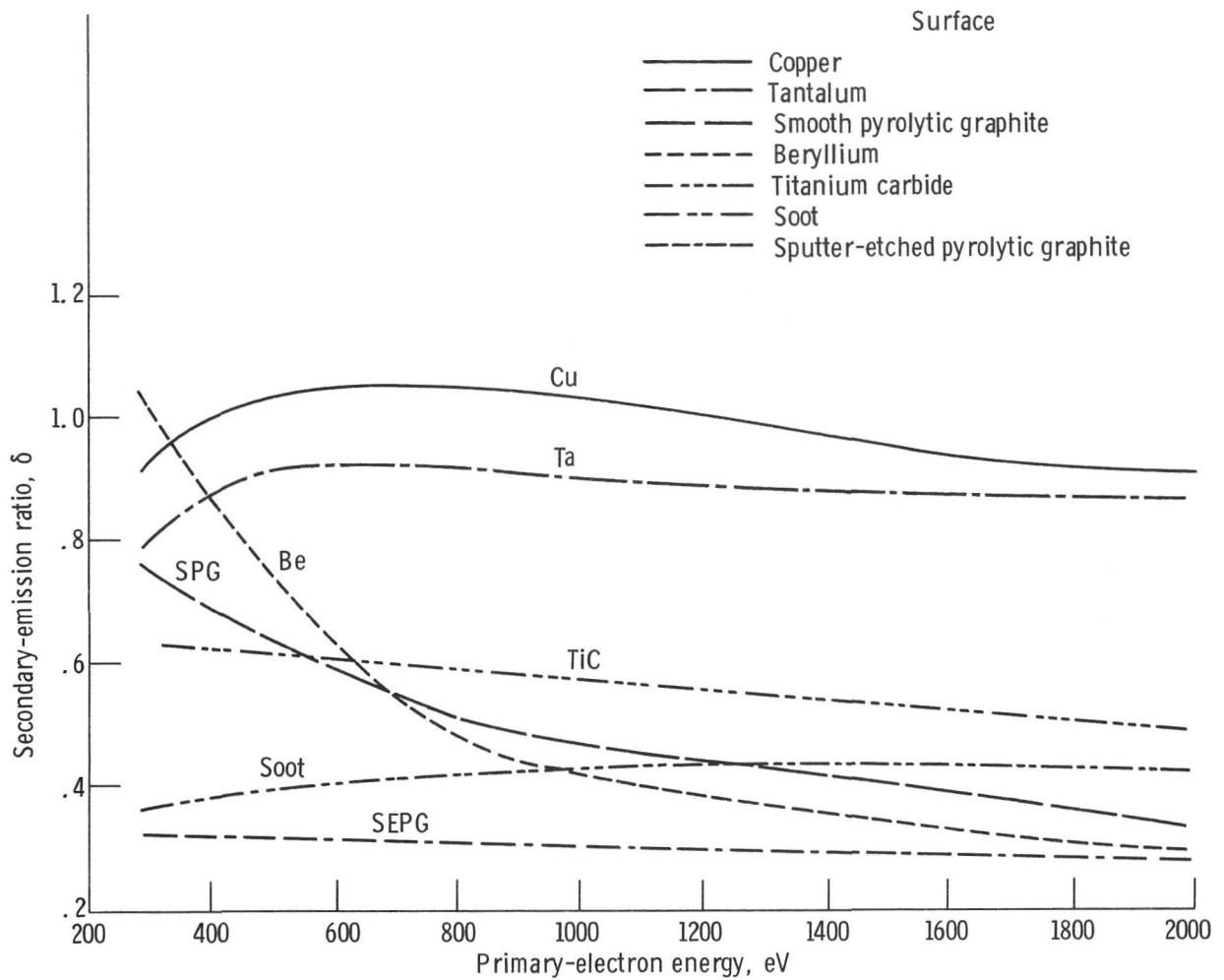
Figure 23. - Secondary-emission ratio as function of primary-electron energy for beryllium, copper, pyrolytic graphite, soot, titanium carbide, and tantalum surfaces in range 300 to 2000 eV.
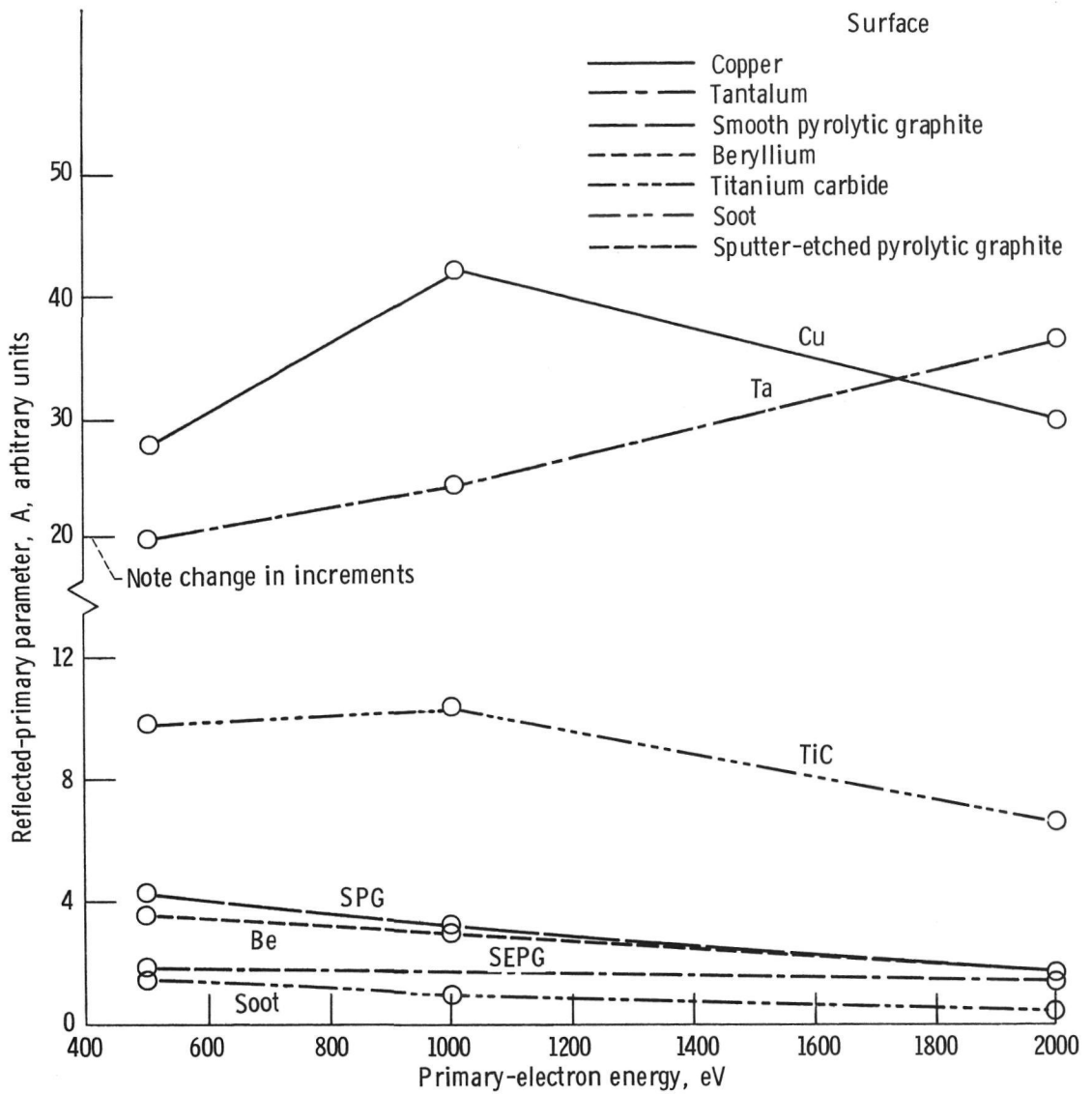
Figure 24. – Reflected-primary parameter A as function of primary-electron energy for beryllium copper, pyrolytic graphite, soot, titanium carbide, and tantalum surfaces in range 500 to 2000 eV.

E-9233

1. Report No. NASA TP-1097	2. Government Accession No.	3. Recipient's Catalog No.
4. Title and Subtitle SECONDARY-ELECTRON-EMISSION PROPERTIES OF CONDUCTING SURFACES WITH APPLICATION TO MULTISTAGE DEPRESSED COLLECTORS FOR MICROWAVE AMPLIFIERS		5. Report Date November 1977
		6. Performing Organization Code
7. Author(s) Ralph Forman		8. Performing Organization Report No. E-9233
		10. Work Unit No. 506-20
9. Performing Organization Name and Address National Aeronautics and Space Administration Lewis Research Center Cleveland, Ohio 44135		11. Contract or Grant No.
		13. Type of Report and Period Covered Technical Paper
12. Sponsoring Agency Name and Address National Aeronautics and Space Administration Washington, D.C. 20546		14. Sponsoring Agency Code

15. Supplementary Notes

16. Abstract

To improve the efficiency of high-power microwave tubes, low-secondary-electron-yield electrode surfaces for use in depressed collectors are needed. The secondary-emission characteristics of a number of materials that were considered likely prospects to accomplish this objective were investigated. The materials studied were beryllium, carbon (soot and pyrolytic graphite), copper, titanium carbide, and tantalum. Both total secondary yield δ (ratio of total secondary current to total primary current) and relative reflected-primary yield were measured. These measurements were made in conjunction with Auger spectroscopy so that the secondary-emission characteristics could be determined as a function of surface contamination or purity. The results show that low-atomic-weight elements, such as beryllium and carbon, have the lowest reflected-primary yield and that roughening the surface of an electrode can markedly decrease secondary yield both for δ and reflected primaries. All factors considered, a roughened pyrolytic graphite surface shows the greatest potential for use as an electrode surface in depressed collectors.

17. Key Words (Suggested by Author(s)) Microwave tubes Secondary emission	18. Distribution Statement Unclassified - unlimited STAR Category 26		
19. Security Classif. (of this report) Unclassified	20. Security Classif. (of this page) Unclassified	21. No. of Pages 31	22. Price* A03